

Progress in functional studies of transition metal borides

Teng Ma(马腾), Pinwen Zhu(朱品文), and Xiaohui Yu(于晓辉)

Citation: Chin. Phys. B, 2021, 30 (**10**): 108103. DOI: 10.1088/1674-1056/ac1925
Journal homepage: http://cpb.iphy.ac.cn; http://iopscience.iop.org/cpb

What follows is a list of articles you may be interested in

Super deformability and thermoelectricity of bulk *γ*-InSe single crystals

Bin Zhang(张斌), Hong Wu(吴宏), Kunling Peng(彭坤岭), Xingchen Shen(沈星辰), Xiangnan Gong(公祥南), Sikang Zheng(郑思康), Xu Lu(卢旭), Guoyu Wang(王国玉), and Xiaoyuan Zhou(周小元)

Chin. Phys. B, 2021, 30 (**7**): 078101. DOI: 10.1088/1674-1056/abf133

A low-dimensional crystal growth model on an isotropic and quasi-free sustained substrate

Chenxi Lu(卢晨曦), Senjiang Yu(余森江), Lingwei Li(李领伟), Bo Yang(杨波), Xiangming Tao(陶向明), Gaoxiang Ye(叶高翔)

Chin. Phys. B, 2020, 29 (**3**): 038101. DOI: 10.1088/1674-1056/ab6968

Study on the nitridation of *β*-Ga_2O_3 films

Fei Cheng(程菲), Yue-Wen Li(李悦文), Hong Zhao(赵红), Xiang-Qian Xiu(修向前), Zhi-Tai Jia(贾志泰), Duo Liu(刘铎), Xue-Mei Hua(华雪梅), Zi-Li Xie(谢自力), Tao Tao(陶涛), Peng Chen(陈鹏), Bin Liu(刘斌), Rong Zhang(张荣), You-Dou Zheng(郑有炓)

Chin. Phys. B, 2019, 28 (**8**): 088103. DOI: 10.1088/1674-1056/28/8/088103

Optical properties of wavelength-tunable green-emitting color conversion glass ceramics

Yang Li(李杨), Li-Li Hu(胡丽丽), Bo-Bo Yang(杨波波), Ming-Ming Shi(石明明), Jun Zou(邹军)

Chin. Phys. B, 2017, 26 (**12**): 128103. DOI: 10.1088/1674-1056/26/12/128103

Structural and photoluminescence studies on europium-doped lithium tetraborate ($Eu:Li_2B_4O_7$) single crystal grown by microtube Czochralski (μT-Cz) technique

A Kumaresh, R Arun Kumar, N Ravikumar, U Madhusoodanan, B S Panigrahi, K Marimuthu, M Anuradha

Chin. Phys. B, 2016, 25 (**5**): 058105. DOI: 10.1088/1674-1056/25/5/058105

REVIEW

Progress in functional studies of transition metal borides*

Teng Ma(马腾)[1,2], Pinwen Zhu(朱品文)[1,†], and Xiaohui Yu(于晓辉)[2,‡]

[1] State Key Laboratory of Superhard Materials, College of Physics, Jilin University, Changchun 130012, China
[2] Beijing National Laboratory for Condensed Matter Physics and Institute of Physics, Chinese Academy of Sciences, Beijing 100190, China

(Received 19 May 2021; revised manuscript received 20 July 2021; accepted manuscript online 30 July 2021)

In recent years, transition metal borides (TMBs) have attracted much attention because they are considered as potential superhard materials and have more abundant crystal structures compared with traditional superhard materials. So far, however, no superhard materials have been found in TMBs. A large number of structures and potential new properties in TMBs are induced by the various hybridization ways of boron atoms and the high valence electrons of transition metals, which provide many possibilities for its application. And most TMBs have layered structures, which make TMBs have the potential to be a two-dimensional (2D) material. The 2D materials have novel properties, but the research on 2D TMBs is still nearly blank. In this paper, the research progress of TMBs is summarized involving structure, mechanical properties, and multifunctional properties. The strong covalent bonds of boron atoms in TMBs can form one-dimensional, two-dimensional, and three-dimensional substructures, and the multiple electron transfer between transition metal and boron leads to a variety of chemical bonds in TMBs, which are the keys to obtain high hardness and multifunctional properties of TMBs. Further research on the multifunctional properties of TMBs, such as superconductors, catalysts, and high hardness ferromagnetic materials, is of great significance to the discovery of new multifunctional hard materials.

Keywords: transition metal borides, crystal structure, hardness, multifunctional properties

PACS: 81.05.Je, 71.20.Be, 91.60.Ed, 62.20.−x **DOI:** 10.1088/1674-1056/ac1925

1. Introduction

Transition metal borides, carbides and nitrides are of great interest in both fundamental science and technical applications.[1–3] In 2005, Kaner *et al.* suggested that, in addition to the existence of superhard materials in the traditional covalent crystals, transition metal borides, carbides, and nitrides may have high hardness and even superhard materials.[4] Henceforth, there has been a new surge of research interest in searching for ultra-incompressible and superhard transition-metal (TM) borides, carbides, and nitrides. Transition metals have high valence electron density and high ultra-incompressibility. The covalent bond between the light elements has a high shear modulus. Preparing borides, carbides, and nitrides with transition-metals may result in a compound with high ultra-incompressible and hardness. Transition-metal borides, carbides, and nitrides have not only covalent bonds, but also ionic bonds and metallic bonds. Thus, transition-metal borides, carbides, and nitrides also have other properties, such as thermal, electrical, magnetic, and so on.

Boron is a special element. Boron, as an electron-deficient element, can not only form a variety of covalent bond hybridization ways (sp1, sp2, sp3) but also has the ability to gain and lose electrons. Thus, boron and transition-metals can form rich and varied compounds. And transition-metal borides (TMBs) can also form rich and varied crystal structures. Transition-metal borides not only have good mechanical properties but also perform well in thermal, electrical and magnetic fields. So far, a great deal of investigation has been carried out on TMBs, which have been found to have abundant crystal structures, and most of the TMBs are high hardness materials. At the same time, some new functions have been explored on this basis, and a preliminary understanding of its multifunction has been obtained.

In this paper, the research progress of transition metal borides in recent years is summarized from three aspects: structure, versatility, and synthesis.

2. The crystal structure of transition metal borides

There are abundant compounds of TMBs with a wide variety of crystal structures. Boron is a unique element. Boron sits at the boundary between metals and nonmetals on the periodic table, which allows it to gain and lose electrons. Transition metals have high electron density and can form abundant valence states. Boron and transition metal can form covalent

*Project supported by the National Key Research and Development Program of China (Grant Nos. 2016YFA0401503 and 2018YFA0305700), the National Natural Science Foundation of China (Grant No. 11575288), the Strategic Priority Research Program and Key Research Program of Frontier Sciences of the Chinese Academy of Sciences (Grant Nos. XDB33000000, XDB25000000, and QYZDBSSW-SLH013), and the Youth Innovation Promotion Association of the Chinese Academy of Sciences (Grant No. Y202003).

†Corresponding author. E-mail: zhupw@jlu.edu.cn
‡Corresponding author. E-mail: yuxh@iphy.ac.cn

© 2021 Chinese Physical Society and IOP Publishing Ltd

bond, metal bond, and ionic bond. In the TMBs, boron atoms can exist in four structural types: isolated boron atom, one-dimensional (1D) boron chain, 2D boron structure, and three-dimensional (3D) boron structure. Isolated boron atoms are commonly found in TMBs with a higher proportion of transition metals, such as Cr_2B and Mo_2B.[5,6] This paper mainly introduces the structures of transition metal borides in four classes: monoboride (TMB), diboride (TMB_2), tetraboride (TMB_4), and dodecaboride (TMB_{12}).

2.1. Transition metal monoborides

In monoborides, there are three main types of crystal structure, namely CrB-type, β-FeB-type, and α-MoB-type. The crystal structure of transition metal monoborides is shown in Fig. 1. The crystal structure of CrB, β-FeB, and α-MoB belong to the orthorhombic with space group *Cmcm* (No. 63),[7] the orthorhombic with space group *Pnma* (No. 62),[8] and the tetragonal with space group *I*41/*amd* (No. 141),[9] respectively. The main difference between the three crystal structures is the position of the boron zigzag chain. In CrB, boron zigzag chains are parallel along the *a* axis. There are seven monoborides belonging to the CrB-type structure, which are respectively VB, CrB, α-FeB, NiB, β-MoB, TaB, and β-WB. The boron zigzag chains of β-FeB are similar to those of CrB in that they are parallel along the *a* axis, but the inclination of boron zigzag chain is different. The structure of TiB, MnB, β-FeB, CoB, and IrB is β-FeB-type. In contrast to CrB, α-MoB possesses the perpendicular boron zigzag chain skeleton. So far, only two monoborides with α-MoB-type structure have been found, namely α-MoB and α-WB.

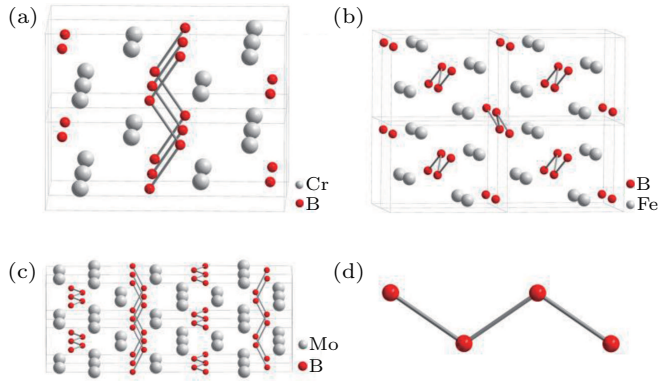


Fig. 1. Structure of monoborides: (a) the crystal structure of CrB; (b) crystal structure of β-FeB; (c) crystal structure of α-MoB; (d) boron atom chain. Boron atoms are in red, metal atoms are in gray.

2.2. Transition metal diborides

The structures of diborides can be roughly classified into five structural types: AlB_2-type, β-MoB_2-type, RuB_2-type, α-WB_2-type, and ReB_2-type. The crystal structure of transition metal diborides is shown in Fig. 2. Boron atoms form 2D boron layers or quasi-3D wrinkled boron layers in these structures. Among diborides, the number of TMB_2 with AlB_2-type structure is the largest.[10] So far, twelve of TMB_2 with AlB_2-type structure have been prepared, namely, ScB_2, TiB_2, VB_2, CrB_2, MnB_2, YB_2, ZrB_2, NbB_2, α-MoB_2, HfB_2, TaB_2, and α-WB_2. In the AlB_2-type structure, boron atoms form graphite-like boron layers and transition metal atoms compose close-packed layers. Each transition metal atom sits at the center of a regular hexagon of boron atoms. Each boron atom has six nearest neighbor transition metal atoms which form a trigonal prism. The boron layer and the transition metal layer alternately arranged.

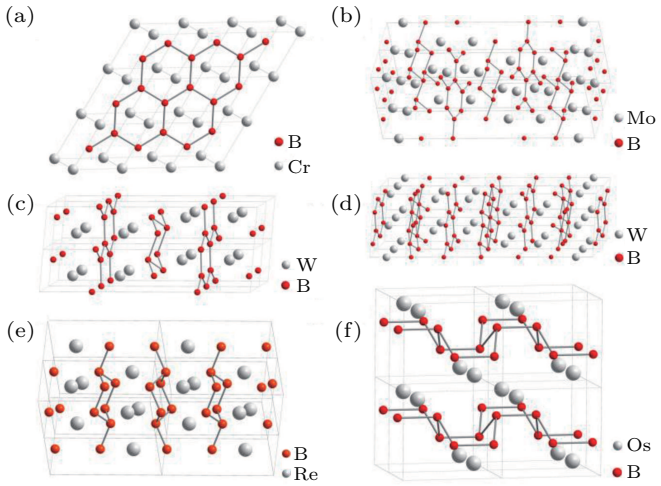


Fig. 2. Structure of diborides: (a) the crystal structure of CrB_2; (b) crystal structure of β-MoB_2; (c) crystal structure of WB_2; (d) crystal structure of W_2B_5; (e) crystal structure of ReB_2; (f) crystal structure of OsB_2. Boron atoms are in red, metal atoms are in gray.

Among the TMB_2 structures, other structures can be considered as modifications of the AlB_2-type structure. The alternating arrangement of boron and transition metal layers is the same, but the 2D structural units that boron atoms form are different. In these structures, boron atoms form a quasi-3D wrinkled boron layer, which is mainly caused by the amount of charge transfer and the directivity of the B–B covalent bond. In the structure of β-MoB_2, there are two kinds of structure units: graphene-like boron layer and wrinkled boron layer, which also arranged alternately.[11] Different from the boron layer in the β-MoB_2 structure, the boron atom formation in the RuB_2 structure is pseudo-hexagonal corrugated boron layers.[12] Only RuB_2, OsB_2, and IrB_2 have RuB_2-type structure.[12,13] The boron layers of ReB_2 are all quasi-3D wrinkled boron layers, which is due to the special electron structure of rhenium formed a special electron transfer.[12,14–19] This quasi-3D boron structure has an important effect on the properties of ReB_2, which makes it more difficult to compress in the *c*-axis direction.[20]

There are some controversies about the structure of MnB_2, MoB_2, and WB_2. Manganese diboride has two crystal structures, AlB_2-type and ReB_2-type. Theoretical calculations showed that the ReB_2-type MnB_2 was more stable

than the AlB_2-type MnB_2 and was predicted to be a superhard material,[21,22] but only AlB_2-type MnB_2 was synthesized experimentally up to now.[23] MoB_2 has two phases with α-MoB_2 and β-MoB_2. The theoretical calculations suggest the α-MoB_2, which has a hexagonal crystal structure with space group *P*6/*mmm* (No. 191), is thermodynamically unstable.[24–27] But the α-MoB_2 was obtained in the experiment and is stable structures at ambient conditions. β-MoB_2 was originally considered to be the Mo_2B_5-type structure.[28,29] Okata *et al.* firstly reported that the ratio of molybdenum atom and boron atom is 1:2 in Mo_2B_5, which is actually β-MoB_2.[30] β-MoB_2 has a rhombohedral crystal structure with *R*-3*m* (No. 166) symmetry. As with the same group element molybdenum, the crystal structure of WB_2 also has the so-called W_2B_5 phase. So far, three crystal structures of WB_2 were reported in the experiment, Mo_2B_5-type (*R*-3*m*), AlB_2-type (*P*6/*mmm*), and W_2B_4-type (*P*63/*mmc*).[31–41] However, the phonon calculations suggested the AlB_2-type WB_2 is dynamically unstable and was predicted to be a stable high-pressure phase above 65 GPa.[33] Another controversy is the stoichiometric ratio of W_2B_5.[42–44] Frotscher *et al.* reported that W_2B_5 is actually W_2B_4 (WB_2) with a space group of *P*63/*mmc* (No. 194),[45] in which the crystal structures and composition were probed by x-ray diffraction (XRD), neutron diffraction, energy dispersive spectrometer (EDS), WDS, scanning electron microscope (SEM), and so on.

2.3. Transition metal tetraborides

In the past few years, TMB_4 was paid attention extensively, because CrB_4, MnB_4, and FeB_4 were considered as potential superhard materials.[21,46–54] The crystal structure of CrB_4, MnB_4, and FeB_4 has many similarities, they all have a 3D network structure. The crystal structure of CrB_4, MnB_4, and FeB_4 is shown in Figs. 3(a), 3(b), and 3(c). The crystal structure of CrB_4 belongs to the orthorhombic. Initially, CrB_4 was described in the space group of *Immm* (No. 71),[46,55] but the theoretical calculation shown that the *Pnnm* (No. 58) phase of CrB_4 is more stable.[48,49,56,57] According to the results of XRD and TEM, Niu *et al.* believed the space group of CrB_4 is *Pnnm* (No. 58).[48] Wang *et al.* reported that the structural difference between *Immm* and *Pnnm* is the site of the boron atom.[58] The powder x-ray and neutron diffraction patterns of *Immm* and *Pnnm* structures were simulated for CrB_4. The results showed that XRD of *Immm* and *Pnnm* structures are the same, the neutron diffraction peaks are the difference. The structural controversy of CrB_4 can be resolved by neutron diffraction. The structure of FeB_4 is similar to that of CrB_4. The symmetry of FeB_4 obtained by the experiment is *Pnnm* (No. 58),[59] which is in agreement with the theoretical calculation results.[60] MnB_4 was initially described in the space group of *C*2/*m* (No. 12).[61] The theoretical calculation suggests that the structure of MnB_4 should be similar to that of CrB_4 and FeB_4, but the experimental results show that the structure of MnB_4 is monoclinic with the space group of $P2_1/c$ (No. 11).[52,62–64] This is mainly due to Peierls distortion, which causes the Mn–Mn atom dimers to appear in the MnB_4 structure and thus distort the MnB_4 crystal structure.

The crystal structure of MoB_4 and WB_4 is also a controversial issue. Theoretically, the structure of WB_4 was considered to be thermodynamically unstable.[65] Some studies suggested that the reported WB_4 is probably stoichiometric WB_3. Although they have the same hexagonal crystal structure with *P*63/*mmc* (No. 194) symmetry,[66] the structure of WB_3 is more stable in theory.[67,68] But Li *et al.* reported that the structure of WB_4 and WB_3 are thermodynamically stable and should be accessible to synthesis.[69] Because the boron atom is small, it is difficult that the site of boron atoms is detected by x-ray diffraction. The symmetry of WB_4 and WB_3 is the same, thereby the x-ray diffraction diagram is similar except for diffraction peak strength. The difference in the crystal structure of WB_4 and WB_3 is the boron–boron dimer. There is the boron–boron dimer in WB_4. Cheng *et al.* reported that the results of Ac-HRTEM experiments suggested boron–boron dimer does not exist,[70] so WB_3 was confirmed to exist. The crystal structure of WB_4 (WB_3) is shown in Fig. 3(d). Some other studies indicated that tungsten atom is the deficiency in WB_3, the chemical formula of WB_3 should be $W_{1-x}B_3$.[71] The crystal structure of reported WB_4 (WB_3) needs further investigations in theory and experiments. The crystal structure of MoB_4 is very similar to WB_4. The reported MoB_4 is not actually stoichiometric MoB_4.[72,73] The general formula can be written as $Mo_{1-x}B_3$, for example, $Mo_{0.8}B_3$ and $Mo_{0.91}B_3$. The crystal structure of $Mo_{1-x}B_3$ is consistent with that of WB_4 in Fig. 3(d). In addition, the calculations suggested that the *R*-3*m* structure of ReB_4 is thermodynamically stable, but so far ReB_4 has not been prepared.[74]

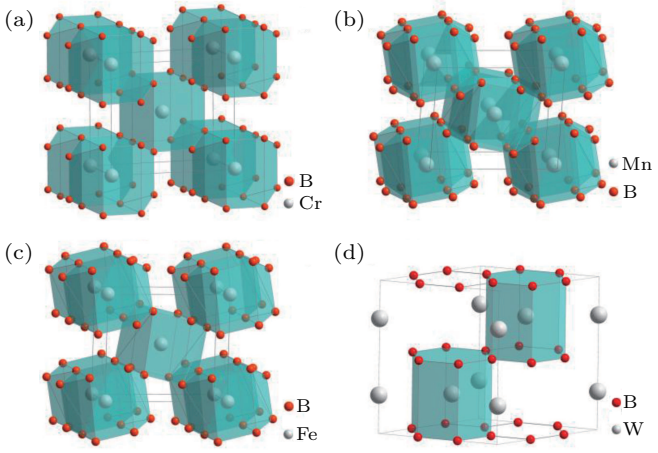


Fig. 3. Structure of tetraborides: (a) the crystal structure of CrB_4; (b) crystal structure of MnB_4; (c) crystal structure of FeB_4; (d) crystal structure of WB_3. Boron atoms are in red, metal atoms are in gray.

2.4. Transition metal dodecaborides

The crystal structure of transition metal dodecaborides (TMB_{12}) can be divided into two structural types: UB_{12}-type crystal structure,[75] which is the majority of TMB_{12} structure, and ScB_{12}-type crystal structure,[76] to which only ScB_{12} belongs. The crystal structure of UB_{12}-type and ScB_{12}-type are shown in Fig. 4. In both types of crystal structures, there are the same structural units in which TM atoms are surrounded by B_{24} cages. In the UB_{12}-type structure, the structural unit of B_{24} cages and TM atoms form the face-centered cubic structure, while in the ScB_{12}-type structure, the structural unit of B_{24} cages and TM atoms form the body-centered tetragonal structure. In addition, B_{12} clusters also exist in both structures. The crystal structure of UB_{12}-type is the same as that of NaCl, with B_{12} clusters at the Na sites and TM atoms at the Cl sites. Interestingly, the structure of both B_{24} cages and B_{12} clusters is cuboctahedral networks.

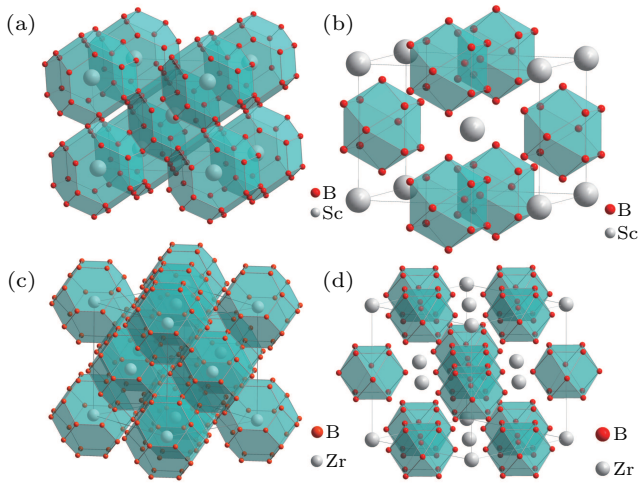


Fig. 4. Structure of dodecaborides: (a) the crystal structure of ScB_{12} with polyhedron of B_{24} cuboctahedra; (b) crystal structure of ScB_{12} with polyhedron of B_{12} cluster; (c) crystal structure of ZrB_{12} with polyhedron of B_{24} cuboctahedra; (d) crystal structure of ZrB_{12} with polyhedron of B_{12} cluster. Boron atoms are in red, metal atoms are in gray.

3. The multifunctional transition metal borides

Superhard materials are the material with Vickers hardness (H_V) above 40 GPa. The most representative superhard materials are diamond and cubic boron nitride (cBN). However, both diamond and cBN have their own disadvantages. The thermal stability of diamond is poor, and diamond is easy to react with Fe-based materials. The hardness of cBN is lower than diamond, and the single crystal is prone to cleavage leading to damage. Therefore, it has always been an urgent need to find alternatives to superhard materials. Boron, carbon, nitrogen, and transition metals can form materials with high valence electron density, strong covalent bonds, and 3D crystal structure, which are the potential superhard materials. In 2007, ReB_2 was reported as a superhard material with a hardness of 48 GPa under a load of 0.49 N by Chung *et al.*[20] This result sets off a new upsurge in the study of TMBs. In addition, TMBs are rich in crystal structure and can form the different amounts of charge transfer between transition metal and boron atoms, which determines the abundant properties of TMBs. This greatly expands the application range of TMBs.

3.1. Mechanical properties

The ReB_2 is particularly noticeable. Base on the first-principle calculations, Hao *et al.* reported the mechanical properties of ReB_2.[77] Chung *et al.* reported that ReB_2 was a superhard material experimentally.[20] So ReB_2 was widely concerned. This is the beginning of the search for superhard materials in TMBs. The hardness of ReB_2 is mainly due to the existence of wrinkle boron layers in the crystal structure of ReB_2, which is a quasi-3D structure. However, asymptotic hardness is the true hardness of a material. ReB_2 only exhibited superhard property ($H_V \geq 40$ GPa) under a load of 0.49 N.[20,78] The Vickers hardness of ReB_2 is 31 GPa under a load of 4.9 N. The Vickers hardness of ReB_2 is shown in Fig. 5. Gu *et al.* reported that the hardness of ReB_2 is $\sim$ 27 GPa under a load of 4.9 N,[79] but Qin *et al.* reported that the hardness of ReB_2 is only 18.4 GPa under a load of 4.9 N.[80] This result is consistent with the theoretical calculation of Yang *et al.*[81] The hardness difference of ReB_2 is $\sim$ 13 GPa under a load of 4.9 N. This is mainly influenced by some extrinsic factors, such as boron content. Because it is usually necessary to add excess boron to prepare the sample, this allows excess boron in the product. Levine *et al.* reported that the excess boron distributed through the compact drastically reduces the hardness of the materials.[82] Because of the excess boron powder compact of ReB_2, the hardness is substantially reduced. Actually, the effect of amorphous boron on the hardness of polycrystalline TMBs is still needed to be further investigated because amorphous boron also has a high hardness. The hardness of the single crystal is the intrinsic hardness of the sample. So far, although the hardness of singlecrystal of ReB_2 has been reported, there are not the asymptotic hardness values under the high load.

Although ReB_2 is not a superhard material, hardness greater than 25 GPa is rare in layered structures. According to previous reports, TMBs with 3D boron atomic structure are more likely to have high hardness. The high hardness of ReB_2 is mainly due to the wrinkled boron layer in its structure, which reflects the quasi-3D effect. This is also reflected in other TMB_2. MoB_2 has two phases with α-MoB_2 and β-MoB_2. The crystal structure of α-MoB_2 is AlB_2-type with space group *P6/mmm* (No. 191). The asymptotic Vickers hardness of α-MoB_2 is $\sim$ 15 GPa. β-MoB_2 has a rhombohedral crystal structure with *R*-3*m* (No. 166) symmetry, and its asymptotic Vickers hardness is $\sim$ 22 GPa. The graphite-like

boron layers in α-MoB_2 can transfer to puckered boron layers in β-MoB_2 with enhanced the Vickers hardness of 7 GPa.[11]

In the OsB_2 structure, boron atoms form another quasi-3D boron layer, a pseudo-hexagonal corrugated boron layer. The investigations suggest that the Vickers hardness of RuB_2-type OsB_2 reaches 37 GPa under a load of 0.245 N.[83] The value is close to the standard of superhard materials ($H_V \geq$ 40 GPa). Hebbache *et al.* reported that RuB_2-type OsB_2 showed an asymptotic hardness of $\sim$ 29 GPa,[84] but Gu *et al.* reported that RuB_2-type OsB_2 showed only an asymptotic hardness of $\sim$ 17 GPa.[79] Although the hardness of RuB_2-type OsB_2 is a quite difference, both indicated that RuB_2-type OsB_2 is not a superhard material under high load. The investigations suggested that the hardness of RuB_2-type OsB_2 is highly dependent on the crystallographic orientation. The average hardness along the $\langle 100 \rangle$ direction is significantly higher than that in the orthogonal $\langle 001 \rangle$ direction. This is attributed to the stronger B–B bonds found along the $\langle 100 \rangle$ direction, which dominate the dislocation motion.[85] There have been many studies on the compressibility of RuB_2-type OsB_2 in experiments and theories,[33,86–91] and the results showed the bulk modulus of RuB_2-type OsB_2 was in the range of 365 GPa–395 GPa.[85,92] The compressibility of RuB_2-type OsB_2 is also anisotropy. The *c* direction of the crystal is the most incompressible. It is interesting that the incompressibility of RuB_2-type OsB_2 along the *c* axis is even larger than the analogous linear incompressibility of diamond.[84] This is because RuB_2-type OsB_2 belongs to the orthogonal crystal system with space group *Pmmn* (No. 59),[12,93] under the external force, the Os atom and B atoms squeeze each other, so that the electrostatic repulsion between atoms reaches the maximum value, thereby increasing the incompressibility of the *c* axis. The RuB_2-type OsB_2 exhibits metallic property, but there is a covalent bond of B–B and Os–B that leads to a high hardness, which is generated by the superposition of the d-electron layer of the Os and the p-electron layer of B.

High boron phases tend to form quasi-3D or 3D structures and thus exhibit high hardness, but some low boron phases also exhibit good hardness. These results provide a deeper understanding of the hardness mechanism of materials. Han *et al.* report that the higher Vickers hardness of CrB ($\sim$ 20 GPa)[7] compared to CrB_2 ($\sim$ 16 GPa)[58] is mainly attributed to the strong 3D Cr–B and zigzag B–B bonding networks in CrB. The results indicate that the monoborides can have better mechanical behavior than the diborides counterparts. The boron content is hence not necessary criteria for the design of hard and superhard materials. The Vickers hardness of CrB and CrB_2 is shown in Fig. 5. The symmetrical electronic partition of the 3D Cr–B and zigzag B–B bonding networks is the reason why CrB can have higher bulk moduli than CrB_2 and CrB_4. The asymptotic Vickers hardness of MnB, Mn_3B_4, and MnB_2 are $\sim$ 16 GPa,[94] $\sim$ 16 GPa,[95] and $\sim$ 12 GPa,[23] respectively. Similar to CrB, MnB and Mn_3B_4 have a higher hardness than that of MnB_2 due to the covalent zigzag or double zigzag B_1–B_2–B_1 backbone. The experimental results indicated the asymptotic Vickers hardness of α-MoB (18.4 GPa) is higher than that of β-MoB (12.2 GPa).[9] Although the crystal structure of α-MoB and β-MoB has the boron zigzag chain (Bzc) skeletons (Bzcs), it is a different arrangement. The Bzcs of α-MoB has a higher shear modulus, and a higher grain boundary density, which resists the glide of dislocation. The results demonstrated modulating the covalent bond array and grain boundary density can also create high hardness in the low-boron content TMBs.

WB_4 is the first tetraboride to be synthesized, and its hardness exceeds 40 GPa under 0.49-N load,[96] which has attracted a lot of attention. But the asymptotic Vickers hardness of WB_4 was in the range of 28 GPa–32 GPa.[79,96,97] The crystal structure of WB_4 does not exist, it should actually be WB_3. The calculation indicated that the asymptotic hardness of WB_4 (WB_3) is lower than that of ReB_2 ($\sim$ 27 GPa).[79,98,99] Boron was excessive in reported experiments to prepare WB_4 (WB_3), and the hardness of amorphous boron is above 30 GPa,[100] so the reported hardness of WB_4 (WB_3) could be influenced by excess amorphous boron. If the hardness of WB_4 (WB_3) is to be obtained, the effects of amorphous boron must be excluded. Tao *et al.* restudied the hardness of WB_3 and found that the hardness of WB_3 excluding the effect of amorphous boron is just 25.5 GPa,[100] which is really lower than that of ReB_2. The asymptotic hardness of WB_3 is exhibited in Fig. 5.

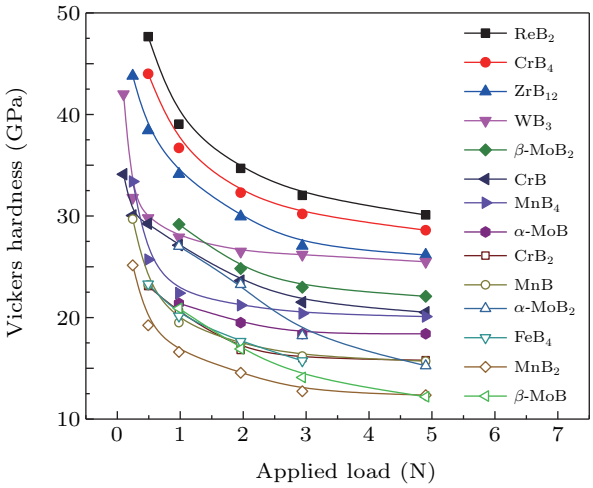


Fig. 5. The hardness of ReB_2, CrB_4, ZrB_{12}, WB_3, β-MoB_2, CrB, MnB_4, α-MoB, CrB_2, MnB, α-MoB_2, FeB_4, MnB_2, and β-MoB (Refs. [7,9,11,20,23,58,59,94,100,101,103]).

Theoretical calculation showed that the Cr, Mn, Fe, and B in CrB_4, MnB_4, and FeB_4 are covalently bonded to form a strong 3D network like as diamond. So there could be superhard materials in these materials. However, the asymptotic Vickers hardness of CrB_4 is only $\sim$ 30 GPa.[58] The Vickers

hardness of CrB_4 is shown in Fig.5. Although it is the highest hardness of the Cr–B system, CrB_4 is not a superhard material. The reasons why CrB_4 with 3D crystal structure do not show superhard property are quantum-mechanical effect involving a transition between two-center and three-center bonding among the boron atoms that reduces the rigidity and directionality of the boron bonding and mechanistic effect caused by the pressure beneath the indenter that drives a lateral bond and volume expansion that further stretches and weakens the boron bonds in addition to the shear deformation in the CrB_4 structure under Vickers indentation hardness tests.[50] Gou *et al.* reported that the Vickers hardness of MnB_4 is $\sim$ 37 GPa under a load of 9.8 N,[64] but this value remains controversial. Knappschneider *et al.* also reported the nanoindentation hardness of MnB_4 with $\sim$ 25 GPa,[63] which is well consistent with the reported by Ma *et al.*, which the polycrystalline hardness of MnB_4 is about 20.1 GPa.[101] FeB_4 was reported to be superhard materials with a hardness of 62 GPa.[102] However, the other measurements of the hardness of FeB_4 indicate that FeB_4 is not a superhard material. Its asymptotic hardness is only 15.4 GPa, which is consistent with the calculated hardness (18.4 GPa).[59] The Vickers hardness of FeB_4 is shown in Fig.5. Although this is still a contentious issue about its hardness, the point can be sure that FeB_4 is not a superhard material.

The higher boron content of transition metal dodecaborides also forms the 3D structures, and the presence of B_{12} clusters in the structure suggests that TMB_{12} are likely to exhibit superhard properties. The hardness of both ZrB_{12} and ScB_{12} exceeds 40 GPa at 0.49-N load,[103,104] but unfortunately does not show superhard properties at high loads. The hardness of ZrB_{12} and ScB_{12} is 27 GPa[103] and 28 GPa[104] at 5 N, respectively. The Vickers hardness of ZrB_{12} is shown in Fig. 5. The hardness of the single crystal of ZrB_{12} is lower than that of polycrystalline samples. This may be caused by the effect of grain boundary in the polycrystalline samples.

3.2. Electrical properties

So far, most of the TMBs prepared are conductors, some of which have excellent conductivity comparable to good metal conductors even in the high boron phase. ZrB_{12} exhibits superior metallic behavior with ultralow electrical resistivity ($\sim$ 18 $\mu\Omega$·cm)[103] at room temperature, which is comparable to that of Pt ($\sim$ 20 $\mu\Omega$·cm). The reason why zirconium dodecaboride shows metallic behavior is the extensive B–B covalent network in ZrB_{12} can form delocalized π-bonds, which generate extensive conducting channels for valence electrons by contacting Zr 4d orbitals.

With the discovery of superconductivity of MgB_2,[105] the electrical transport properties of TMBs have been paid more attention. So far, there are many TMBs with superconducting properties. The crystal structure of MgB_2 is AlB_2-type, but only ZrB_2 has been reported to have superconductivity with $T_c = 5.5$ K among the AlB_2-type TMB_2.[106] However, these results were not observed in later studies. Stoichiometric NbB_2 does not show superconductivity, but NbB_{2+x} with excess boron does show superconductivity with a critical temperature of 8.9 K–11 K.[107,108] Like NbB_{2+x}, adding excess boron to MoB_2 will make it exhibits superconductivity. MoB_{2+x} also was reported to show superconductivity at $T_c \approx 7.5$ K.[108] Tang *et al.* reported that a boron-rich molybdenum boride, the large single-crystal of nonstoichiometry molybdenum triboride ($Mo_{0.757}B_3$), was prepared under high-pressure high-temperature conditions, it exhibits superconductivity with a T_C of 2.4 K.[110] The analysis of theoretical calculations indicated that the occurrence of its superconductivity is derived from the partial occupancy of Mo atoms. MoB_4 is not a superconductor, but the Ti-doped and Nb-doped MoB_4 were found to be superconducting near 6 K to 8 K.[111] Renosto *et al.* reported that the $Zr_{0.96}V_{0.04}B_2$ specimen exhibited bulk superconductivity at a critical temperature of 8.7 K and explained that the superconductivity of the $Zr_{0.96}V_{0.04}B_2$ specimen was related to multiple bands at the Fermi surface.[112,113] Gou *et al.* reported the experiment results that FeB_4 shows the bulk superconductivity below 2.9 K.[102] However, the later experimental investigation showed that FeB_4 did not exhibit the bulk superconductivity for temperature as low as 2.5 K.[59] FeB_4 shows a metallic behavior from room temperature to 30 K. Further investigation is still needed for bulk superconductivity of FeB_4. TMB_{12} with higher boron content has also been found to have superconductivity, such as ScB_{12} (0.39 K),[114] YB_{12} (4.7 K),[115,116] and ZrB_{12} (5.8 K).[103,117–120]

3.3. Catalysis

Energy and environment are the most important issues involved in the sustainable development of human society. Fossil fuels are a non-renewable resource, and their use will bring about environmental pollution, and the development of clean energy has become an urgent practical demand. Electrochemical water splitting is an important method for preparing clean fuel hydrogen with water, but the preparation of hydrogen is difficult and generally requires a catalyst. The most effective electrocatalysts are Pt-based materials for the hydrogen evolution reaction (HER), but the high cost and low earth abundance of noble metal based catalyst limit their wide use. It is very important to develop well-working nonprecious metal based electrocatalysts for HER.

α-MoB_2 is a superefficient electrocatalyst for the HER and has excellent catalytic stability during HER.[121–124] It was demonstrated by Chen *et al.* that α-MoB_2 efficiently catalyzes

the HER, even at large current densities.[125] The theoretical and experimental results suggested the catalytic activity of α-MoB_2 is due to its excellent conductivity, a large density of efficient catalytic active sites, and good mass transport properties. β-MoB_2 is also the efficient electrocatalyst for HER, but the catalytic activities of β-MoB_2 is lower than that of α-MoB_2. In the Mo-B system, α-MoB_2 is the most efficient catalyst for the HER. All the tungsten borides have the catalytic activity for the HER. Like α-MoB_2, W_2B_4-type WB_2, which has the same crystal structure with α-MoB_2, is also the most efficient catalyst for the HER in the W–B system.[126,127]

3.4. Magnetic properties

With the rapid development of micro-electromechanical systems devices, magnetic sensors, high-speed motors, and magnetic springs, new requirements are put forward for ferromagnetic materials. The low hardness of traditional magnetic materials, such as Fe (1.4 GPa),[128] Fe_3O_4 (4 GPa),[129] FeNi (4 GPa),[130] *etc.*, inevitably limits the application of traditional magnetic materials in harsh conditions. The demand for strong ferromagnetic materials with high hardness is constantly enhanced. Although the hardness of TMBs does not reach the hardness of superhard materials, most TMBs reach the hardness of cemented carbide. MnB exhibits high Curie temperature (546 K), high saturated magnetization (155.5 emu/g), and low coercive field (H_c = 15.9 Oe, 1 Oe = 79.5775 $A{\cdot}m^{-1}$).[94] The coercive field of MnB indicates that it is a soft magnetic material. The asymptotic Vickers hardness of MnB is $\sim$ 16 GPa, which is far higher than that of traditional ferromagnetic materials. Fe_2B also exhibits ferromagnetism and the Curie temperature (1017 K) is comparable to that of Fe (1043 K). The asymptotic Vickers hardness of Fe_2B (12.4 GPa) is far higher than that of traditional ferromagnetic materials.[131] Fe_2B is a promising candidate for strong ferromagnetic and high hardness material.

3.5. Refractory materials

Refractory materials are widely used in industrial fields, such as aerospace, geological exploration, machinery manufacturing, *etc.* The majority of TMBs are refractory. ZrB_2 has been widely paid attention to due to its excellent refractory properties. ZrB_2 has a hexagonal crystal structure with the space group of *P6/mmm* (No. 191). Because ZrB_2 has strong covalent B–B bonds, its melting point has a very high temperature of 3245 °C.[132–134] ZrB_2 also shows outstanding oxidation resistance, surviving thermal cycling up to 2700 °C in air.[135] The thermal conductivity (k) of ZrB_2 is its notable property. Kinoshita *et al.* reported that room-temperature k values for single crystals are 140 $W{\cdot}(m{\cdot}K)^{-1}$ along the c axis and 100 $W{\cdot}(m{\cdot}K)^{-1}$ along the a axis.[136] Lonergan *et al.* reported the high temperature thermal conductivity of ZrB_2, which shows thermal conductivity of 127 $W{\cdot}(m{\cdot}K)^{-1}$ at 298 K and 80 $W{\cdot}(m{\cdot}K)^{-1}$ at 2273 K.[137] Besides, the high temperature flexure strengths of ZrB_2 was measured by Neuman *et al.* The investigations indicated that strength between room temperature and 1200 °C was $\sim$ 390 MPa, decreasing to a minimum of $\sim$ 170 MPa between 1400 °C and 1500 °C and the strength increased to $\sim$ 220 MPa between 1600 °C and 2300 °C.[138] The increase in strength was mainly attributed to stress relief through plastic flow. As a kind of high temperature resistant material, ZrB_2 has been used in the aerospace field.

4. Preparation of transition metal borides

The study of the physical properties of materials is inseparable from the preparation of materials. After years of development, there are many methods for the preparation of TMBs. Because transition metals and boron have very high melting points, and TMBs, especially the high boron phase, have strong covalent bonds, most preparation methods require high temperatures. At present, the synthesis methods of transition metal borides mainly include arc melting, solid-state sintering, high pressure and high temperature (HPHT), and so on.

Arc melting is one of the earliest and most widely used methods for synthesizing transition metal borides. Arc melting is conducted in a water-cooled copper hearth, with high purity argon as the protective gas, in which an electrode made of a material with a high melting point generates a high-temperature arc to melt and react the sample. Most TMBs with different boron contents can be synthesized by arc melting, such as MnB_4, ReB_2, WB_4, and YB_{12}, *etc.*[20,96,139,140]

Solid-state sintering is a widely used synthesis method, and can also be used to prepare TMBs. This method is relatively simple. Boron and transition metal powders are mixed in a certain proportion and sintered in a vacuum or an inert atmosphere to obtain the target products. But the drawbacks are also obvious. Due to the limitation of heating materials in equipment, this method is insufficient in preparing high boron phase, and the synthesis time is relatively long. Frotscher *et al.* reported that MoB_2 was synthesized at 1373 K in an inert atmosphere within 14 d.[45] In the experiment, ball milling the precursor or adding fluxing agents is used to reduce the reaction temperature and increase the reaction rate.

Compared with other synthetic methods, HPHT has advantages in the synthesis of TMBs. In addition to the temperature, the HPHT method adds another adjustable parameter pressure. High pressure can shorten the distance between atoms, increase electron cloud overlap, and facilitate the formation of strong chemical bonds. So HPHT is the main way to synthesize diamond and cubic boron nitride. In addition, HPHT is also beneficial to the preparation of bulk materials with high density. This is very convenient to research the properties of bulk TMBs, like mechanical properties and electrical

properties. Although many preparation methods can provide high temperatures, the presence of high pressures greatly facilitates the synthesis of TMBs. It takes 14 d–28 d to prepare the single crystal of MnB_4 by solid-state sintering,[63] but only one hour to get a single crystal of MnB_4 by HPHT.[64] In addition, HPHT can also obtain specimens that cannot be obtained by other methods. Studies have shown that it is difficult to prepare FeB_4 under 3 GPa,[102] and the current reported preparation pressure of FeB_4 is 10 GPa–15 GPa.[59] It can be seen that HPHT has more advantages in exploring new materials and new structures.

In addition, high-temperature electrochemistry, electron beam melting, spark plasma sintering, self-propagating sintering, magnetron sputtering, pulsed laser deposition, high-frequency induction, and floating zone can also be used to prepare TMBs. Magnetron sputtering and pulsed laser deposition are mainly used to prepare thin film samples. High-frequency induction and floating zone are often used to prepare single crystal samples.[141,142]

The synthetic routes of TMBs are also abundant. After boron purification technology is mature, the preparation of TMBs is mainly obtained by the reaction of boron and transition metal.[95,96] The chemical equation is as follows:

$$x\mathrm{TM} + y\mathrm{B} \rightarrow \mathrm{TM}_x\mathrm{B}_y.$$

In addition, there are other synthetic routes, such as:

1) Borothermal reduction of transition metal oxides[143]

$$\mathrm{TMO} + \mathrm{B} \rightarrow \mathrm{TMB} + \mathrm{BO}.$$

2) Solid state metathesis of borides[144]

$$\mathrm{TMCl}_x + \mathrm{MgB}_2 \rightarrow \mathrm{TMB}_y + \mathrm{MgCl}_2.$$

3) Carbothermal reduction[145]

$$\mathrm{TMO} + \mathrm{B_2O_3} + \mathrm{C} \rightarrow \mathrm{TMB} + \mathrm{CO}.$$

4) Boron carbide reduction of transition metal oxides[146]

$$\mathrm{TMO} + \mathrm{B_4C} \rightarrow \mathrm{TMB} + \mathrm{B_2O_3} + \mathrm{CO}.$$

5) Hydrothermal reaction in an autoclave[147]

$$\mathrm{TMCl_4} + \mathrm{NaBH_4} \rightarrow \mathrm{TMB_2} + \mathrm{NaCl} + \mathrm{HCl} + \mathrm{H_2}.$$

Some are actually ways to synthesize nanomaterials. Because most synthetic routes are not preparation methods of bulk materials, they will not be listed here. Although there are many ways to synthesize TMBs at present, there are still many problems in the preparation of TMBs. Some TMBs do not readily form a single phase. For example, the synthesis of CrB_4 is usually accompanied by the phase of CrB_2.[58] The synthesis of FeB_4 is also accompanied by the phase of FeB.[59] The synthesis of some transition metal borides requires an excess of boron, which affects the study of some properties.

5. Summaries

After more than 100 years of development, transition metal borides (TMBs) have obtained abundant crystal structure and physical properties experimentally. However, the research on TMBs is far from complete, and there are still many problems to be further studied. So far, the hardness of the synthesized TMBs is not ideal, and there is still a certain gap with the superhard materials. This is mainly because the TMBs have some metal bonds, so the number of covalent bonds is reduced, and the covalent bonds in the TMBs are not strong in direction, and the bonding strength is not enough. Therefore, the research on the hardness of TMBs needs to be improved in the material design concept. The key to the design and preparation of high hardness TMBs is to increase the electron transfer between the transition metal and boron atoms and to construct a network of quasi-3D or 3D strong covalent bonds. At present, the research on TMBs mainly focuses on crystal structure, mechanical properties and oxidation resistance and so forth, and many potential multifunction properties have not been explored in depth, such as strong ferromagnetic materials and electrocatalytic materials. Among all kinds of TMBs preparation methods, the HPHT method has unique advantages for the preparation of TMBs, which can effectively induce the electron transfer between the transition metal and boron atoms, so as to construct a more abundant crystal structure, and is an effective method for the preparation of hard multi-functional new TMBs materials. TMBs are still a candidate material for studying new materials, new structures, and new properties due to the existence of multiple electron transfer modes between boron and transition metal. In the future research of TMBs, one is to design and prepare TMBs with high hardness, and the other is to strengthen the research and development of other multifunction properties. In addition, there are a lot of layer structures in TMBs, which are the basis for studying two-dimensional materials. Therefore, in recent years, two-dimensional materials for the study of TMBs begin to rise. For example, the two-dimensional MoB has been prepared,[148] which greatly expands the research scope of TMBs.

References

[1] Jhi S, Ihm J, Louie S G and Cohen M L 1999 *Nature* **399** 132
[2] Ivanovskii A L 2011 *J. Superhard Mater.* **33** 73
[3] Yeung M T, Mohammadi R and Kaner R B 2016 *Ann. Rev. Mater. Res.* **46** 465
[4] Kaner R B, Gilman J J and Tolbert S H 2005 *Science* **308** 1268
[5] Zhou C T, Xing J D, Xiao B, Feng J, Xie X J and Chen Y H 2009 *Comp. Mater. Sci.* **44** 1056
[6] Iyer A K, Zhang Y, Scheifers J P *et al.* 2019 *J. Solid State Chem.* **270** 618
[7] Han L, Wang S M, Zhu J L, *et al.* 2015 *Appl. Phys. Lett.* **106** 221902
[8] Jeffries J B and Hershkowitz N 1969 *Phys. Lett. A* **30** 187
[9] Tao Q, Chen Y L, Lian M, Xu C H, Li L, Feng X K, Wang X, Cui T, Zheng W T and Zhu P W 2018 *Chem. Mater.* **31** 200
[10] Vajeeston P, Ravindran P, Ravi C and Asokamani R 2001 *Phys. Rev. B* **63** 045115

[11] Tao Q, Ma Y M, Li Y, Chen Y L, Ma Y M, Cui T, Wang X and Zhu P W 2013 *RSC Adv.* **4** 52878
[12] Frotscher M, Hölzel M and Albert B 2010 *Z. Anorg. Allg. Chem.* **636** 1783
[13] Wang D Y, Wang B and Wang Y X 2012 *J. Phys. Chem. C* **116** 21961
[14] La Placa S J and Post B 1962 *Acta Crystallogr.* **15** 97
[15] Zhou W, Wu H and Yildirim T 2007 *Phys. Rev. B* **76** 184113
[16] Zhao E J, Wang J P, Meng J and Wu Z J 2010 *J. Comput. Chem.* **31** 1904
[17] Xie M, Winkler B, Mao Z, Kaner R B, Kavner A and Tolbert S H 2014 *Appl. Phys. Lett.* **104** 011904
[18] Koumoulis D, Turner C L, Taylor R E and Kaner R B 2016 *J. Phys. Chem. C* **120** 2901
[19] Deligoz E, Colakoglu K and Ciftci Y O 2012 *Chin. Phys. B* **21** 106301
[20] Chung H Y, Weinberger M B, Levine J B, Cumberland R W, Kavner A, Yang J M, Tolbert S H and Kaner R B 2007 *Science* **316** 436
[21] Wang B, Li X, Wang Y X and Tu Y F 2011 *J. Phys. Chem. C* **115** 21429
[22] Aydin S and Simsek M 2009 *Phys. Rev. B* **80** 134107
[23] Ma S L, Bao K, Tao Q, Xu C H, Feng X D, Zhu P W and Cui T 2016 *Inorg. Chem.* **55** 11140
[24] Zhang M G, Wang H, Wang H B, Cui T and Ma Y M 2010 *J. Phys. Chem. C* **114** 6722
[25] Liang Y C, Yuan X, Fu Z, Li Y and Zhong Z 2012 *Appl. Phys. Lett.* **101** 181908
[26] Liang Y C, Wu Z B, Yuan X, Zhang W Q and Zhang P H 2016 *Nanoscale* **8** 1055
[27] Rybkovskiy D V, Kvashnin A G, Kvashnina Y A and Oganov A R 2020 *J. Phys. Chem. Lett.* **11** 2393
[28] Higashi I, Takahashi Y and Okada S 1986 *J. Less-Common Met.* **123** 277
[29] Klesnar H, Aselage T L, Morosin B and Kwei G H 1996 *J. Alloys Compd.* **241** 180
[30] Okada S, Atoda T, Higashi I and Takahashi Y 1987 *J. Mater. Sci.* **22** 2993
[31] Woods H P, Wawner F E, Jr. and Fox B G 1966 *Science* **151** 75
[32] Okada S, Kudou K and Lundström T 1995 *Jpn. J. Appl. Phys.* **34** 226
[33] Chen X Q, Fu C L, Krcmar M and Painter G S 2008 *Phys. Rev. Lett.* **100** 196403
[34] Jiang C L, Pei Z L, Liu Y M, Xiao J Q, Gong J and Sun C 2013 *Phys. Status Solidi A Appl. Mater.* **210** 1221
[35] Lech A T, Turner C L, Lei J, Mohammadi R, Tolbert S H and Kaner R B 2016 *J. Am. Chem. Soc.* **138** 14398
[36] Liu Y M, Han R Q, Liu F, Pei Z L and Sun C 2017 *J. Alloys Compd.* **703** 188
[37] Turner C L, Zujovic Z, Koumoulis D, Taylor R E and Kaner R B 2017 *J. Phys. Chem. C* **121** 1315
[38] Henschel A, Binnewies M, Schmidt M, Köppe R, Burkhardt U and Grin Y 2018 *Chem-Eur. J.* **24** 10109
[39] Long Y, Wu Z, Zheng X, Lin H T and Zhang F L 2019 *J. Am. Ceram. Soc.* **103** 831
[40] Ma K, Xue X X and Cao X Z 2019 *Int. J. Appl. Ceram. Tec.* **17** 1177
[41] Che J T, Long Y, Zheng X, Lin H T and Plucknett K 2019 *Mater. Chem. Phys.* **237** 121848
[42] Armas B and Trombe F 1973 *Solar Energy* **15** 67
[43] Stadler S, Winarski R P, MacLaren J M, Ederer D L, vanEk J, Moewes A, Grush M M, Callcott T A and Perera R C C 2000 *J. Electron Spectrosc.* **110–111** 75
[44] Feng S Q, Yang Y, Li J Y, Jiang X X, Li H N and Cheng X L 2017 *Mod. Phys. Lett. B* **31** 1750137
[45] Frotscher M, Klein W, Bauer J, Fang C M, Halet J F, Senyshyn A, Baehtz C and Albert B 2007 *Z. Anorg. Allg. Chem.* **633** 2626
[46] Knappschneider A, Litterscheid C, Kurzman J, Seshadri R and Albert B 2011 *Inorg. Chem.* **50** 10540
[47] Gou H Y, Li Z P, Niu H, Gao F M, Zhang J W, Ewing R C and Lian J 2012 *Appl. Phys. Lett.* **100** 111907
[48] Niu H Y, Wang J Q, Chen X Q, Li D Z, Li Y Y, Lazar P, Podloucky R and Kolmogorov A N 2012 *Phys. Rev. B* **85** 144116
[49] Knappschneider A, Litterscheid C, Dzivenko D, Kurzman J A, Seshadri R, Wagner N, Beck J, Riedel R and Albert B 2013 *Inorg. Chem.* **52** 540
[50] Li B, Sun H, Zang C P and Chen C F 2013 *Phys. Rev. B* **87** 174106
[51] Zhao W J and Xu B 2012 *Comp. Mater. Sci.* **65** 372
[52] Niu H Y, Chen X Q, Ren W J, Zhu Q, Oganov A R, Li D Z and Li Y Y 2014 *Phys. Chem. Chem. Phys.* **16** 15866
[53] Ding L P, Kuang X Y, Shao P and Huang X F 2014 *Inorg. Chem.* **53** 3471
[54] Wang Q Q, Zhang Q, Hu M, Ma M D, Xu B and He J L 2014 *Phys. Chem. Chem. Phys.* **16** 22008
[55] Andersson S, Lundström T, Andresen A F and Pearson W B 1968 *Acta Chem. Scand.* **22** 3103
[56] Wang B, Wang D Y, Cheng Z X, Wang X L and Wang Y X 2013 *ChemPhysChem* **14** 1245
[57] Li X H, Cui H L and Zhang R Z 2017 *Chin. Phys. B* **26** 096201
[58] Wang S M, Yu X H, Zhang J, Zhang Y, Wang L P, Leinenweber K, Xu H W, Popov D, Park C, Yang W, He D W and Zhao Y S 2014 *J. Superhard Mater.* **36** 279
[59] Wang Q Q, He J L, Hu W T, Zhao Z S, Zhang C, Luo K, Lü Y F, Hao C X, Lü W M, Liu Z Y, Yu D L, Tian Y J and Xu B 2015 *J. Materiomics* **1** 45
[60] Kolmogorov A N, Shah S, Margine E R, Bialon A F, Hammerschmidt T and Drautz R 2010 *Phys. Rev. Lett.* **105** 217003
[61] Andersson S, Carlsson J O, Astrup E E, Liaaen-Jensen S, Lamvik A, Sunde E and Sørensen N A 1970 *Acta Chem. Scand.* **24** 1791
[62] Litterscheid C, Knappschneider A and Albert B 2012 *Z. Anorg. Allg. Chem.* **638** 1608
[63] Knappschneider A, Litterscheid C, George N C, Brgoch J, Wagner N, Beck J, Kurzman J A, Seshadri R and Albert B 2014 *Angew. Chem. Int. Ed.* **53** 1684
[64] Gou H Y, Tsirlin A A, Bykova E, Abakumov A M, Van Tendeloo G, Richter A, Ovsyannikov S V, Kurnosov A V, Trots D M, Konôpková Z, Liermann H P, Dubrovinsky L and Dubrovinskaia N 2014 *Phys. Rev. B* **89** 064108
[65] Liang Y C, Yuan X and Zhang W Q 2011 *Phys. Rev. B* **83** 220102
[66] Duschanek H and Rogl P 1995 *J. Phase Equilib.* **16** 150
[67] Zhang R F, Legut D, Lin Z J, Zhao Y S, Mao H K and Veprek S 2012 *Phys. Rev. Lett.* **108** 255502
[68] Cheng X Y, Chen X Q, Li D Z and Li Y Y 2014 *Acta Crystallogr. C Struct. Chem.* **70** 85
[69] Li Q, Zhou D, Zheng W T, Ma Y M and Chen C F 2013 *Phys. Rev. Lett.* **110** 136403
[70] Cheng X Y, Zhang W, Chen X Q, Niu H Y, Liu P T, Du K, Liu G, Li D Z, Cheng H M, Ye H Q and Li Y Y 2013 *Appl. Phys. Lett.* **103** 171903
[71] Zeiringer I, Rogl P, Grytsiv A, Polt J, Bauer E and Giester G 2014 *J. Phase Equilib. Diff.* **35** 384
[72] Kiessling R, Wetterholm A, Sillén L G, Linnasalmi A and Laukkanen P 1947 *Acta Chem. Scand.* **1** 893
[73] Lundström T and Rosenberg I 1973 *J. Solid State Chem.* **6** 299
[74] Wang B, Wang D Y and Wang Y X 2013 *J. Alloys Compd.* **573** 20
[75] Troć R, Wawryk R, Pikul A and Shitsevalova N 2015 *Philos. Mag.* **95** 2343
[76] Peshev P, Etourneau J and Naslain R 1970 *Mater. Res. Bull.* **5** 319
[77] Hao X F, Xu Y H, Wu Z J, Zhou D F, Liu X J, Cao X Q and Meng J 2006 *Phys. Rev. B* **74** 224112
[78] Levine J B, Nguyen S L, Rasool H I, Wright J A, Brown S E and Kaner R B 2008 *J. Am. Chem. Soc.* **130** 16953
[79] Gu Q F, Krauss G and Steurer W 2008 *Adv. Mater.* **20** 3620
[80] Qin J Q, He D W, Wang J H, Fang L M, Lei L, Li Y J, Hu J, Kou Z L and Bi Y 2008 *Adv. Mater.* **20** 4780
[81] Yang J, Gao, F M and Liu Y S 2017 *Chin. Phys. B* **26** 106202
[82] Levine J B, Betts J B, Garrett J D, Guo S Q, Eng J T, Migliori A and Kaner R B 2010 *Acta Mater.* **58** 1530
[83] Chung H Y, Yang J M, Tolbert S H and Kaner R B 2008 *J. Mater. Res.* **23** 1797
[84] Hebbache M, Stuparević L and Živković D 2006 *Solid State Commun.* **139** 227
[85] Chung H Y, Weinberger M B, Yang J M, Tolbert S H and Kaner R B 2008 *Appl. Phys. Lett.* **92** 261904
[86] Chiodo S, Gotsis H J, Russo N and Sicilia E 2006 *Chem. Phys. Lett.* **425** 311
[87] Chen Z Y, Xiang H J, Yang J, Hou J G and Zhu Q 2006 *Phys. Rev. B* **74** 012102
[88] Gou H Y, Hou L, Zhang J W, Li H, Sun G F and Gao F M 2006 *Appl. Phys. Lett.* **88** 221904
[89] Yang J, Sun H and Chen C F 2008 *J. Am. Chem. Soc.* **130** 7200

[90] Luo X G, Li J P, Hu P and Dong S L 2010 *Sci. China Technol. Sci.* **53** 1877
[91] Ivanovskii A L 2012 *Inorg. Mater.* **3** 319
[92] Cumberland R W, Weinberger M B, Gilman J J, Clark S M, Tolbert S H and Kaner R B 2005 *J. Am. Chem. Soc.* **127** 7264
[93] Aronsson B, Leden I, Sunner S, Hatanaka A and Munch-Petersen J 1963 *Acta Chem. Scand.* **17** 2036
[94] Ma S L, Bao K, Tao Q, Zhu P W, Ma T, Liu B, Liu Y Z and Cui T 2017 *Sci. Rep.* **7** 43759
[95] Ma S L, Bao K, Tao Q, Xu C H, Feng X K, Zhao X B, Ge Y F, Zhu P W and Cui T 2019 *Phys. Chem. Chem. Phys.* **21** 2697
[96] Mohammadi R, Lech A T, Xie M, Weaver B E, Yeung M T, Tolbert S H and Kaner R B 2011 *Proc. Natl. Acad. Sci.* **108** 10958
[97] Mohammadi R, Xie M, Lech A T, Turner C L, Kavner A, Tolbert S H and Kaner R B 2012 *J. Am. Chem. Soc.* **134** 20660
[98] Zang C P, Sun H, Tse J S and Chen C F 2012 *Phys. Rev. B* **86** 014108
[99] Zang C P, Sun H and Chen C F 2012 *Phys. Rev. B* **86** 180101
[100] Tao Q, Zheng D F, Zhao X P, Chen Y L, Li Q, Li Q, Wang C C, Cui T, Ma Y M, Wang X and Zhu P W 2014 *Chem. Mater.* **26** 5297
[101] Ma S L, Bao K, Tao Q, Huang Y P, Xu C C, Li L, Feng X K, Zhao X B, Zhu P W and Cui T 2019 *Int. J. Refractory Metals Hard Mater.* **85** 104845
[102] Gou H Y, Dubrovinskaia N, Bykova E, Tsirlin A A, Kasinathan D, Schnelle W, Richter A, Merlini M, Hanfland M, Abakumov A M, Batuk D, Van Tendeloo G, Nakajima Y, Kolmogorov A N and Dubrovinsky L 2013 *Phys. Rev. Lett.* **111** 157002
[103] Ma T, Li H, Zheng X, Wang S M, Wang X C, Zhao H Z, Han S B, Liu J, Zhang R F, Zhu P W, Long Y W, Cheng J G, Ma Y M, Zhao Y S, Jin C Q and Yu X H 2017 *Adv. Mater.* **29** 1604003
[104] Akopov G, Yeung M T, Sobell Z C, Turner C L, Lin C W and Kaner R B 2016 *Chem. Mater.* **28** 6605
[105] Nagamatsu J, Nakagawa N, Muranaka T, Zenitani Y and Akimitsu J 2001 *Nature* **410** 63
[106] Gasparov V A, Sidorov N S, Zver'kova I I and Kulakov M P 2001 *JETP Lett.* **73** 532
[107] Escamilla R, Lovera O, Akachi T, Durán A, Falconi R, Morales F and Escudero R 2004 *J. Phys.: Condens. Matter* **16** 5979
[108] Mudgel M, Awana V P S, Bhalla G L and Kishan H 2008 *Solid State Commun.* **147** 439
[109] Cooper A S, Corenzwit E, Longinotti L D, Matthias B T and Zachariasen W H 1970 *Proc. Natl. Acad. Sci.* **67** 313
[110] Tang H, Gao X, Zhang J, Gao B, Zhou W J, Yan B M, Li X, Zhang Q H, Peng S, Huang D J, Zhang L J, Yuan X H, Wan B, Peng C, Wu L L, Zhang D Z, Liu H Y, Gu L, Gao F M, Irifune T, Ahuja R, Mao H K and Gou H Y 2019 *Chem. Mater.* **32** 459
[111] Simonson J W, Wu D, Poon S J and Wolf S A 2010 *J. Supercond. Nov. Magn.* **23** 417
[112] Renosto S T, Consoline H, dos Santos C A M, Albino Aguiar J, Jung S G, Vanacken J, Moshchalkov V V, Fisk Z and Machado A J S 2013 *Phys. Rev. B* **87** 174502
[113] Jung S G, Vanacken J, Moshchalkov V V, Renosto S T, dos Santos C A M, Machado A J S, Fisk Z and Albino Aguiar J 2013 *J. Appl. Phys.* **114** 133905
[114] Matthias B T, Geballe T H, Andres K, Corenzwit E, Hull G W and Maita J P 1968 *Science* **159** 530
[115] Shein I R and Ivanovskii A L 2003 *Phys. Solid State* **45** 1429
[116] Jäger B, Paluch S, ŻogałO J, Wolf W, Herzig P, Filippov V B, Shitsevalova N and Paderno Y 2006 *J. Phys.: Condens. Matter* **18** 2525
[117] Lortz R, Wang Y, Abe S, Meingast C, Paderno Y B, Filippov V and Junod A 2005 *Phys. Rev. B* **72** 024547
[118] Wang Y X, Lortz R, Paderno Y, Filippov V, Abe S, Tutsch U and Junod A 2005 *Phys. Rev. B* **72** 024548
[119] Gasparov V A, Sidorov N S and Zver'kova I I 2006 *Phys. Rev. B* **73** 094510
[120] Ge J Y, Gladilin V N, Sluchanko N E, Lyashenko A, Filipov V B, Indekeu J O and Moshchalkov V V 2017 *New J. Phys.* **19** 093020
[121] Park H, Encinas A, Scheifers J P, Zhang Y and Fokwa B P T 2017 *Angew. Chem. Int. Ed.* **56** 5575
[122] Jothi P R, Zhang Y, Scheifers J P, Park H and Fokwa B P T 2017 *Sustain. Energy Fuels* **1** 1928
[123] Chen Z J, Duan X G, Wei W, Wang S B, Zhang Z J and Ni B J 2020 *Nano Res.* **13** 293
[124] Chen H and Zou X X 2020 *Inorg. Chem. Front.* **7** 2248
[125] Chen Y L, Yu G T, Chen W, Liu Y P, Li G D, Zhu P W, Tao Q, Li Q J, Liu J W, Shen X P, Li H, Huang X R, Wang D J, Asefa T and Zou X X 2017 *J. Am. Chem. Soc.* **139** 12370
[126] Wang Y, Mayorga-Martinez C C, Chia X, Sofer Z, Mohamad Latiff N and Pumera M 2019 *ACS Sustainable Chem. Eng.* **7** 12148
[127] Li Q J, Wang L N, Ai X, Chen H, Zou J Y, Li G D and Zou X X 2020 *Chem. Commun.* **56** 13983
[128] Li X, Li Y, Wei Y H, Hou L F, Liu B S, Qu H B and Wang Y D 2018 *J. Iron Steel Res. Int.* **25** 923
[129] Amano T, Okazaki M, Takezawa Y, Shiino A, Takeda M, Onishi T, Seto K, Ohkubo A and Shishido T 2006 *Mater. Sci. Forum* **522–523** 469
[130] Matsui I, Mori H, Kawakatsu T, Takigawa Y, Uesugi T and Higashi K 2014 *Mater. Sci. Eng. A* **607** 505
[131] Zhao X B, Li L, Bao K, Zhu P W, Tao Q, Ma S L, Liu B, Ge Y F, Li D and Cui T 2020 *Phys. Chem. Chem. Phys.* **22** 27425
[132] Rahman M, Wang C C, Chen W, Akbar S A and Mroz C 1995 *J. Am. Ceram. Soc.* **78** 1380
[133] Fahrenholtz W G, Binner J and Zou J 2016 *J. Mater. Res.* **31** 2757
[134] Kravchenko S E, Kovalev D Y, Korobov I I, Kalinnikov G V, Konovalikhin S V, Khomenko N Y and Shilkin S P 2019 *Inorg. Mater.* **55** 458
[135] Inoue R, Arai Y, Kubota Y, Kogo Y and Goto K 2018 *J. Mater. Sci.* **53** 14885
[136] Kinoshita H, Otani S, Kamiyama S, Amano H, Akasaki I, Suda J and Matsunami H 2001 *Jpn. J. Appl. Phys.* **40** L1280
[137] Lonergan J M, Fahrenholtz W G, Hilmas G E and Trice R 2014 *J. Am. Ceram. Soc.* **97** 1689
[138] Neuman E W, Hilmas G E, Fahrenholtz W G and Dominguez-Rodriguez A 2013 *J. Am. Ceram. Soc.* **96** 47
[139] Cely A, Tergenius L E and Lundstrom T 1978 *J. Less-Common Met.* **61** 193
[140] Akopov G, Roh I, Sobell Z C, Yeung M T and Kaner R B 2018 *Dalton Trans.* **47** 6683
[141] Otani S and Ohsawa T 1999 *J. Cryst. Growth* **200** 472
[142] Werheit H, Filipov V, Shirai K, Dekura H, Shitsevalova N, Schwarz U and Armbruster M 2011 *J. Phys.: Condens. Matter* **23** 065403
[143] Liu Z T, Wei Y N, Meng X, Wei T T and Ran S L 2017 *Ceram. Int.* **43** 1628
[144] Rao L, Gillan E G and Kaner R B 1995 *J. Mater. Res.* **10** 353
[145] McKenna P M 1936 *Ind. Eng. Chem.* **28** 767
[146] Zhao H, He Y and Jin Z Z 1995 *J. Am. Ceram. Soc.* **78** 2534
[147] Chen L Y, Gu Y L, Yang Z H, Shi L, Ma J H and Qian Y T 2004 *Scr. Mater.* **50** 959
[148] Alameda L T, Moradifar P, Metzger Z P, Alem N and Schaak R E 2018 *J. Am. Chem. Soc.* **140** 8833